NRIAG Journal of Astronomy and Geophysics (2014) 3, 7–17

National Research Institute of Astronomy and Geophysics

NRIAG Journal of Astronomy and Geophysics

www.elsevier.com/locate/nrjag

Geophysical assessment of the hydraulic property of the fracture systems around Lake Nasser-Egypt: In sight of polarimetric borehole radar

Khamis Mansour [a], Alhussein A. Basheer [a,*], Taha Rabeh [a], Ahmed Khalil [a], A.A. Essam Eldin [b], Motoyuki Sato [c]

[a] *National Research Institute of Astronomy and Geophysics (NRIAG), 11722 Helwan, Cairo, Egypt*
[b] *Research Institute of Groundwater (RIGW), Kalubia, Egypt*
[c] *Center for Northeast Asian Studies, Tohoku University, Kawauchi, Sendai 980-8576, Japan*

Received 20 August 2013; revised 18 October 2013; accepted 21 January 2014
Available online 22 February 2014

KEYWORDS

Fracture characterization;
Polarimetric borehole radar;
Polarimetric analysis;
Lake Nasser and Nubian aquifer

Abstract Hydraulic property of the subsurface structures is a complicated mission. In this work, the polarimetric analysis for the measured dataset applied by the polarimetric borehole radar system in order to delineate the characteristics of subsurface fractures. Two different locations in USA and Egypt were selected to perform our investigation. The first polarimetric dataset has been acquired at Mirror Lake, USA which is well known as a standard site for testing the hydraulic properties of subsurface fractures (Sato et al., 1999). The results show the presence of nine fracture zones in one borehole FSE-1. The hydraulic properties were detected and the subsurface fractures were differentiated into four categories fracture zones after deriving the radar polarimetric analysis of alpha, entropy and anisotropy parameters at 30 MHz frequency. The fracture zones at 24.75, 47.8 and 55.2 m depths have the highest hydraulic transmissivity while the fracture zones at 28.5, 36.15 m have the lowest hydraulic transmissivity. These results show a good consistency with the hydraulic permeability tracer test and the structures exist in the area.

Similarly, we used the same technique to characterize the subsurface fracture systems detected by geoelectric and geomagnetic methods around Lake Nasser in Egypt using the previous results of Mirror Lake as a key guide. The results show a great correlation with detected structures prevailed in the sedimentary and basement rocks. These results illustrate an ideal explanation for the prevailed subsurface structures and the recharging of the main Nubian sandstone aquifer from Lake Nasser. Also, these results also show that the northeast fracture zone trends are most probably

* Corresponding author. Address: Geomagnetic and Geoelectric Department, National Research Institute of Astronomy and Geophysics (NRIAG), Egypt. Tel.: +20 1122802222; fax: +20 225548020.
E-mail address: Alhussein007@yahoo.com (A.A. Basheer).

Peer review under responsibility of National Research Institute of Astronomy and Geophysics.

ELSEVIER Production and hosting by Elsevier

http://dx.doi.org/10.1016/j.nrjag.2014.01.002

having the highest hydraulic transmissivity whereas the northwest fracture zones have the lowest one.

The integration of surface geophysical measurements with the polarimetric borehole radar and the polarimetric analysis of its datasets introduce better understanding of the recharging mechanism between surface water and the subsurface aquifer and also can be used as clue for identifying the subsurface structures for different areas.

1. Introduction

Flow interaction between a permeable rock and embedded conductive fractures remains poorly understood since earlier research may have investigated only into fractures (Smith, 1993), focused on idealized synthetic fracture geometries (Bogdanov et al., 2003), or applied a dual porosity approach assuming a stagnant matrix (Dershowitz and Miller, 1995; Kazemi, 1993). It is also difficult to monitor fracture flow in experiments (Renard et al., 2001). Using analytical solutions and finite-element analysis, many authors have been also involved to quantify the fracture connectivity, length distribution and saturation variations with layer thickness and lithology affecting and controlling the hydraulic conductivity of crystalline and tight sedimentary rock (Kranz et al., 1979; Taylor et al., 1999; Wu and Pollard, 1995, 2003).

Borehole radar is a special electromagnetic application of ground penetrating radar for determining the depth and location of subsurface fractures depending on their properties and their filled materials. This tool has limitations due to high attenuation of the electromagnetic waves.

In our work we are accommodating the polarimetric radar technology (Sato et al., 1999) to be used for investigating subsurface structures derived from the borehole measurements. To do that using the full polarimetric borehole radar system, a combination of the dipole and slot antennas as transmitter and receiver for acquiring the full polarimetric information for subsurface fractures was used. The dipole antenna transmits or receives the vertical polarized electromagnetic signals and the slot antenna transmits or receives the horizontal polarized ones. The full polarimetric measurements for a single borehole consist of measuring four times with a pair of antennas if the transmitter and receiver are the same type of antenna we call it Co-polarization measurements (VV and HH). On the other hand, when, the antenna pairs are not of same type we call it Cross- polarization measurements (VH and HV).

The configuration of the polarimetric borehole radar system is shown in Fig. 1. The advantage of this system is that: it overcomes the radar resolution as it measures the full polarization states in the borehole for the vertical backscattered and vertical transmitted electromagnetic signals (VV); vertical backscattered and horizontal transmitted signals (VH); horizontal backscattered and vertical transmitted signals (HV) and horizontal backscattered and horizontal transmitted signals (HH). We tested the method for evaluating the parameters of the known subsurface structures of the standard site at Mirror Lake, USA.

We applied this method to define the parameters of known subsurface structures such at Mirror Lake test site then applying the deduced results to estimate the unknown parameters of the subsurface structures previously detected using land magnetic and geoelectric survey around the artificial Lake Nasser, Egypt.

2. Data acquisition and interpretation

2.1. Polarimetric data acquisition at Mirror Lake area, USA

The Mirror Lake test site is a crystalline rock and quite homogeneous except for fracture sets. It is been used in the scientific researches/experiments to study the flow in fractured rocks by the USGS Toxic Substance Hydrology Program since 1990. The joint research group of Tohoku University and USGS carried out the field measurements at Mirror Lake site. These measurements involved a borehole cluster of FSE-1, -2, -3, and -4 (Fig. 2), which form a square (Lane and Haeni, 1998).

The full polarimetric single-hole radar measurements were conducted at FSE-3 and FSE-1 wells, with an antenna separation of 1.6 m. The separation distance between FSE-1 and FSE-3 is 9 m and the frequency-domain of the acquired data was between 2 and 402 MHz with a 2 MHz frequency interval. The single-hole full polarimetric dataset acquired at FSE-1 borehole1 is shown in Fig. 2.

2.2. Theoretical bases of the polarimetric data analysis

We are accommodating the polarimetric analysis to be used for investigating the hydraulic characteristics of subsurface structures derived from the polarimetric borehole radar measurements. The implementation of the target decomposition theorem for subsurface fracture characterization is based on the expected value of the coherency matrix T. The coherency matrix formation is based on the introduction of a scattering vector $\overrightarrow{k}_p$ where this vector can be estimated depending on the scattering matrix S elements $(S_{HH}, S_{HV}, S_{VH}, S_{VV})$ at certain single frequency. The scattering matrix S and scattering vector $\overrightarrow{k}_p$ are defined as follows:

$$S = \begin{bmatrix} S_{HH} & S_{HV} \\ S_{VH} & S_{VV} \end{bmatrix} \tag{1}$$

$$\overrightarrow{k}_p = \frac{1}{\sqrt{2}}[S_{HH} + S_{VV}\ S_{HH} - S_{VV}\ 2S_{HV}]^T \tag{2}$$

The coherency matrix T is formed by averaging the outer product of scattering vector $\overrightarrow{k}_p$ as shown in Eq. (3), the averaging window size can be $(3 \times 3, 5 \times 5$ or $7 \times 7)$, and it has real non-negative eigenvalues and orthogonal eigenvectors.

$$\langle T \rangle = \frac{1}{N}\sum_{i=1}^{N} k_i . k_i^{*T} \tag{3}$$

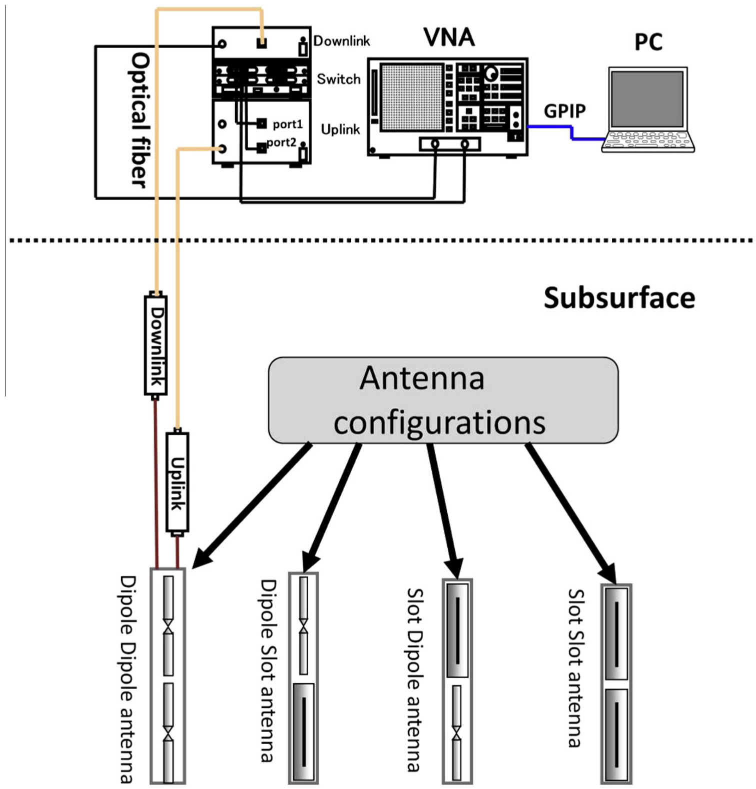

Fig. 1 Schematic shows the configuration of the full polarimetric borehole radar system.

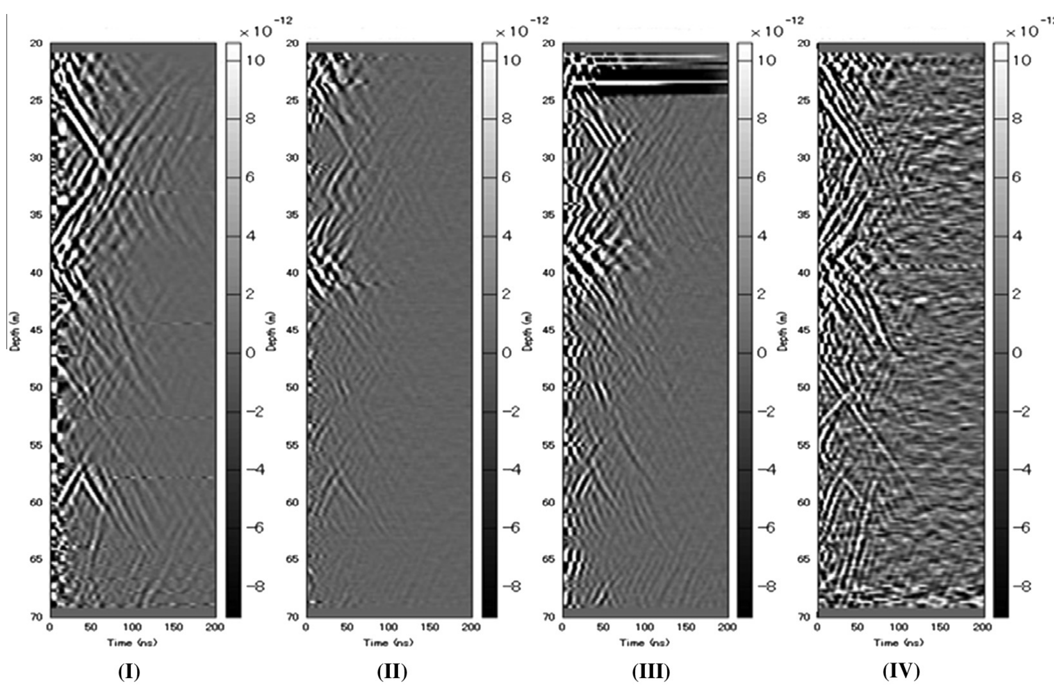

Fig. 2 The full polarimetric borehole radar measurement datasets of FSE1 well at Mirro Lake, USA test site. (I) VV polarization, (II) VH polarization, (III) HV polarization and (IV) HH polarization components.

The coherency matrix can be decomposed into three unitary matrices in order to facilitate calculation of both the eigenvalues and the eigenvectors of the form

$$[T] = [U_3][\Lambda][U_3]^{-1} \quad (4)$$

where $[\Lambda] = \begin{bmatrix} \lambda_1 & 0 & 0 \\ 0 & \lambda_2 & 0 \\ 0 & 0 & \lambda_3 \end{bmatrix}$ and $[U_3] = [\overrightarrow{e_1}, \overrightarrow{e_2}, \overrightarrow{e_3}]^T$ that λ_1, λ_2 and λ_3 are eigenvalues and $\overrightarrow{e_1}$, $\overrightarrow{e_2}$ and $\overrightarrow{e_3}$ are eigenvectors.

Three important physical features are arising directly from the diagonalization of the coherency matrix. The first two are obtained from the eigenvalues of *T*, which normalized by the absolute scattering magnitudes and can be interpreted as scattering probabilities p_i as in Eq. (5). The third one is derived from the eigenvector elements.

$$p_i = \frac{\lambda_i}{\sum_{i=1}^{3} \lambda_i} \quad (5)$$

Based on eigenvalues and eigenvectors of Eq. (4), (Cloude and Pottier, 1997) defined three important parameters for the representation of target information, which are the polarization entropy (*H*), alpha angle (α) and anisotropy (*A*). *H*, α and *A* are defined as follows:

$$H = -\sum_{i=1}^{3} p_i \log_3 p_i \quad (6)$$

$$\alpha = \sum_{i=1}^{3} p_i \alpha_i \quad (7)$$

$$A = \frac{\lambda_2 - \lambda_3}{\lambda_2 + \lambda_3} \quad (8)$$

The three eigenvector decompositions (entropy, anisotropy and alpha) are proved to be effective in terrain surface classification. For that reason, we utilized this decomposition technique for further extract of information about the characteristics of subsurface fractures for the polarimetric radar dataset. In this paper, the three eigenvector decompositions (anisotropy, entropy and alpha) will be used as deterministic parameters and their distributions for susceptibility to fractures with large roughness and fracture zones with severely cracked rock. These parameters evolve the description of scattering mechanism due to fracture properties as they show sensitivity for randomness of fracture surface characteristics.

2.3. Constructing the 3D polarimetric distributions of entropy (H)–anisotropy (A) and alpha (α)

A local region of 2× 1.5 m dimension around each fracture sets was selected to determine the three eigenvectors (entropy–anisotropy–alpha). We were able to monitor nine subsurface sets intersected FSE-1 borehole axis at depths range from 20 to 70 m, which is the borehole radar acquisition interval for the measured data. For the full polarization data (e.g. VV, VH, HV and HH), entropy, anisotropy and alpha were used to characterize the parameters of the subsurface fractures using different frequencies (e.g. 30, 60, 80 and 100 MHz). We observed that high frequency components, above 60 MHz, are less sensitive to evaluate the small fracture surface roughness variation. The results in Fig. 3 show the comparison of the polarimetric analysis for the three eigenvector parameters (entropy–anisotropy–alpha) at 30 and 100 MHz for 28.5, 40.25 and 60 m fracture zones. It is noticed that the distributions of the three eigenvector parameters become unstable at 100 MHz compared to 30 MHz. As, the depolarization effect tends to be large when we use high frequency and the representations of these three parameters (entropy–anisotropy–alpha) have a wider distribution pattern than using the low frequency. Therefore, the eigenvector analysis based on the three eigenvector parameters is determined at 30 MHz.

Fig. 4 shows the 3D distributions for entropy–anisotropy–alpha parameters for all fracture sets at depths 24.75, 28.5, 36.15, 40.25, 42, 44.8, 47.8, 55.2 and 60 m at 30 MHz single frequency. The correlation of *H*, *A* and *alpha* distributions of the fracture sets at 24.75, 47.8 and 55.2 m depths and the hydraulic transmissivity fracture tracer results measured by USGS for FSE-1 borehole, has confirmed that these fracture sets showed the highest hydraulic transmissivity zones ($K = 1 \times 10^{-5}$–1×10^{-7}). Although fracture set at 55.2 m depth has no hydraulic transmissivity data, however, based on its polarimetric distributions, we can deduce that it has the same characteristics with fracture sets at 24.75 and 47.8 m depths. The low hydraulic transmissivity fracture zones are at 28.5, 36.15, 44.8 and 60 m depths ($K = 1 \times 10^{-8}$–1×10^{-9}) and the distribution of the three eigenvectors shows low entropy and anisotropy values as well as low alpha contents. These representations declare low rough fracture zones and small fracture widths.

It can be stated that the relationship between the three polarimetric parameters and fracture characteristics can be elucidated according to the physical meaning of each subsurface structure and the rock fracture type. The entropy (*H*) describes randomness of the electromagnetic scattering mechanisms which is strongly related to the fracture surface roughness (Jone-Sen Lee and Eric Pottier, 2009). When entropy (*H*) has low or medium values we cannot have a clear relation between second and third eigenvalues therefore the anisotropy (*A*) is used to characterize the random scattering from rough fractures depending on the relative magnitudes of the second and third eigenvalues. On the other hand, low values of alphas indicate smooth rough fractures. Based on these results, we can conclude the existence of the direct relationship between the fracture hydraulic transmissivity and the radar polarimertic analysis for subsurface fractures. Table 1 shows the relationship between the fracture type, depth and the determined polarimetric parameters of fracture zone.

3. Application of the polarimetric borehole radar system at Lake Nasser, Egypt

The previous results at Mirror Lake site, USA is used as a key to prove the capability of the polarimetric borehole radar to analyze and delineate the unknown subsurface fracture zones and their hydraulic property prevailing at Lake Nasser area. This site has the Nubian sandstone aquifer that consists of two connected water bearing formations namely Sabaya and Abu Simbel. These two aquifers (water bearings) are hydraulically connected by the faulting system. The expected role of fracture zones which associated with that fault system is important as they control the direction of groundwater trans-

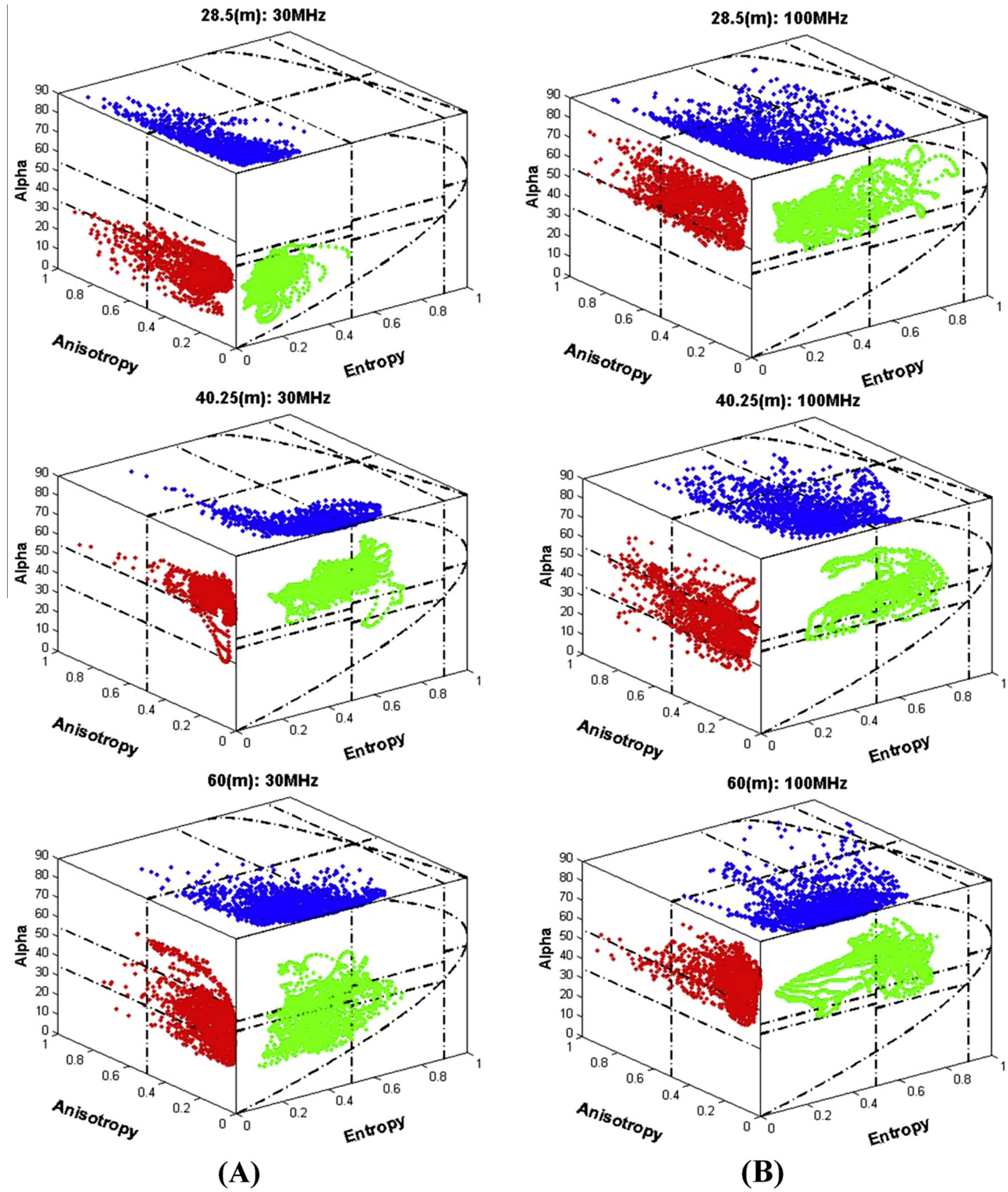

Fig. 3 Comparison of the polarimetric analysis distribution for the three eigenvector decomposition parameters (entropy–anisotropy–alpha) at single frequencies (A) 30 MHz and (B) 100 MHz.

missivity. However, the hydraulic characteristics of that fracture zones are not revealed yet. To do so, a detailed investigation has been applied.

3.1. Tectonic setting and hydrogeology of the Lake Nasser site

The Egyptian Geological Survey and Mining Authority (EGSMA, 1993) showed that the rock distributions around Lake Nasser area belong to the Nubian Formation. The geological map of the southwest Lake Nasser area can be seen in Fig. 5. As, many authors (e.g., Bhattacharyya, 1979; Butzer et al., 1968; Hendriks, 1987; Issawi et al., 1968; El Shazly et al., 1974; Shazly et al., 1976; Van Houten and Klitzsch, 1987) have studied the geology of southwest Lake Nasser region. Their studies indicated that this area consists of a thick sedimentary section of Nubian sandstone formation of upper Cretaceous age that overlies the Precambrian basement rocks. It is known that the Nubian formation is the oldest sedimentary unit exposed and unconformably lies over the Precambrian basement complex (Ghoubashi, 2010). This formation is affected by the structure geology formed in basement complex under it and both of them are tectonically

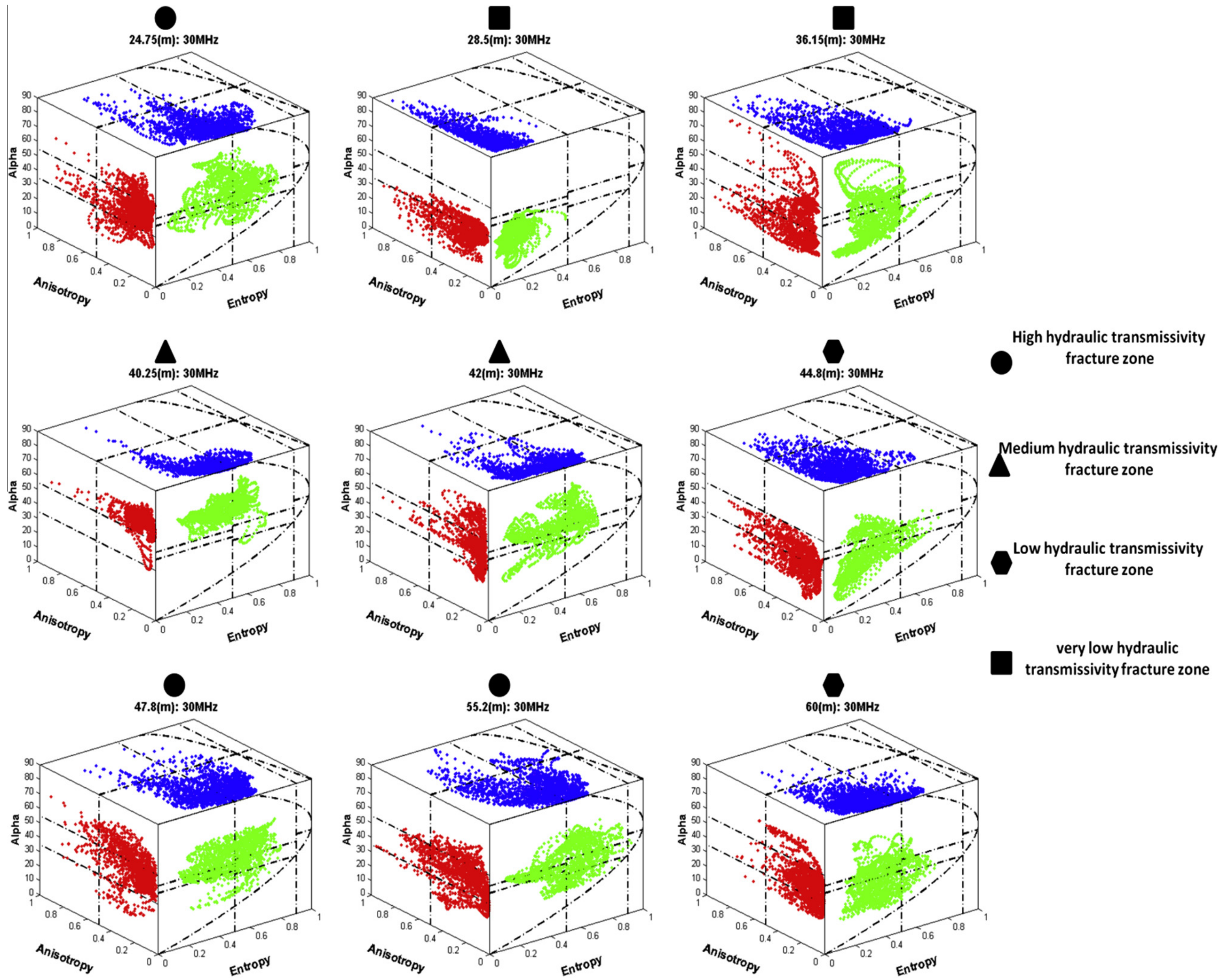

Fig. 4 Hydraulic characterization for nine fracture zones based on entropy, anisotropy and alpha parameters at 30 MHz frequency.

Table 1 The deduced hydraulic characteristics of the nine fracture zones based on entropy, anisotropy and alpha parameters at 30 MHz frequency.

Depth (m)	Deduced fracture type	Entropy (*H*)	Anisotropy (*A*)	Alpha (α)
24.75	High transmissive-connected type	High	High	Moderate (volume scattering)
28.5	Very low transmissive-disconnected type	Low	Low	Low (surface scattering)
36.15	Very low transmissive-disconnected type	Moderate to low	Low	Low (surface scattering)
40.25–42	Transmissive-connected type	High	Low	Moderate to high (volume-double scattering)
44.8	Low transmissive-partially connected type	Moderate to low	Moderate to low	Moderate to low (surface-volume scattering)
47.8	High transmissive-connected type	High	High	Moderate (volume scattering)
55.2	High transmissive-connected type	High	High	Moderate (volume scattering)
60	Low transmissive-partially connected type	Moderate to low	Moderate to low	Moderate to low (surface-volume scattering)

affected by the tectonic stress applied in this area (Issawi et al., 1968).

3.2. Hydrological impact of subsurface fracture zones

The hydrological setting around Lake Nasser and its western margin showed that the Nubian aquifers adjacent to the lake are affected strongly by the faulting systems and their accompanied fracture zones. Thus, the possibility of recharging process of the groundwater aquifers is occurring via these subsurface structures and fracture zones existence from Nasser Lake. Hence, the monitoring of water levels inside the observatory wells at the southwest Aswan area showed a higher water table for few far wells from the lake shore while a lower water table for closer wells.

The hydro-geological information of the southwest Aswan area is obtained from the drilled water wells by the Water Research Center and concluded that the Abu Simbel forma-

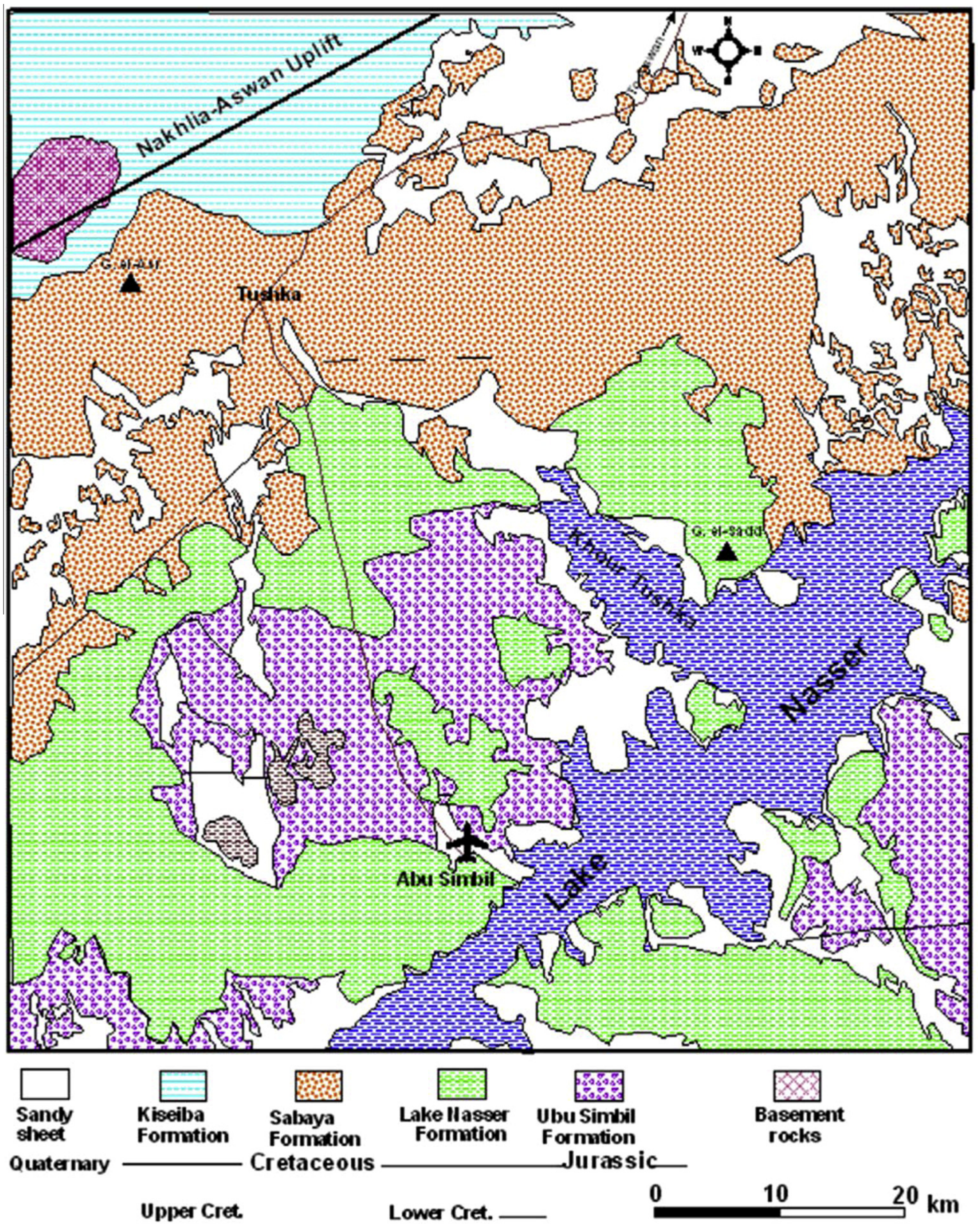

Fig. 5 Geological map of the southwest Nasser Lake area (after CONOCO, 1987).

tion is connected to the surface water of Lake Nasser directly and the Sabaya aquifer has its recharged from the fault plane and its accompanied fracture zones from Abu Simbel formation (Ghoubashi, 2010). However, the role of these fracture zones as a transmissive passes in addition to the direction of water flowing has not be evolved yet.

The variations of water tables in the borehole around Lake Nasser have shown the gradient decrease in water level far away from the lake shore which was reversed in the past (before the presence of Lake Nasser and construction of the High Dam). Furthermore, these changes in water tables are not symmetrical as the effect of subsurface discontinuities, joints and fracture zones (Khalil et al., 2009).

3.3. Geoelectrical measurements and results

The Vertical Electrical Sounding (VES's) survey was carried out at southwest Aswan area in order to determine the structures in subsurface and its relation to the recharge of main aquifer in addition to the geometry and later extension of the Nubian aquifers. The measurements were performed in profile forms to cover the examined area as shown in Fig. 6.

The geological structure and its discontinuity planes such as fault and fracture zones could be provided from the inversion and interpretation of the Vertical Electrical Sounding (VES's) data. These results give insight to the primary connection between the water recharge from Lake Nasser to the groundwater aquifer and the role of subsurface fractures in this process.

The geoelectric section A–A′ as shown in Fig. 7, parallel to Khor Tushka and extending from SE to NW direction, shows that the main aquifer is represented by the saturated Nubian Sandstone. This is considered the lowest resistivity layer, whose resistivity ranges from 70 ohm-m at the southeastern part (near Lake Nasser) to about 180 ohm-m northwest. This

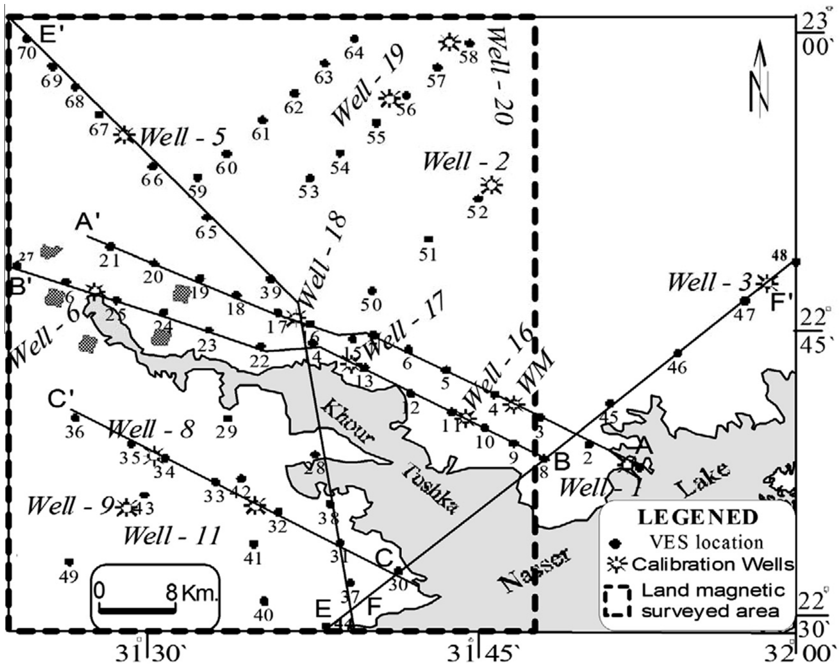

Fig. 6 The sketch map for the VES locations and the derived geoelectric sections, geomagnetic survey region and the drilled boreholes.

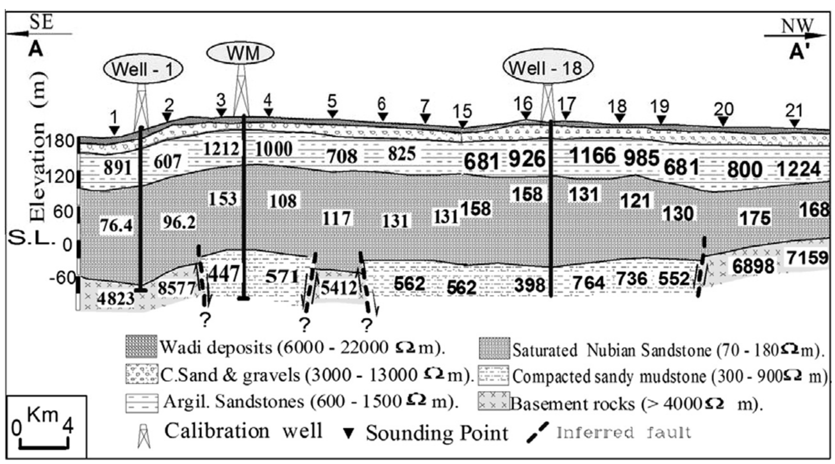

Fig. 7 Geoelectric cross section A–A′ extending perpendicular nearly to the lake shoreline showed the structures in basement complex and overlain Nubian sandstone.

later variation of the resistivity values for the main groundwater aquifer indicates that the water saturation of that aquifer is highly near the Lake Nasser and confirms the occurrence of recharging mechanism from Lake Nasser into Nubian aquifer. This geoelectric section also shows that the basement rock is affected by four fault lines. It was indicated by the sudden appearance of a high resistivity layer whose resistivity reaches more than 7000 ohm-m and these faults affected the overlain Nubian aquifer. As, they lead to the occurrences of fractured aquifer type but the hydraulic properties of that fractures cannot be determined with VES's measurements.

The variation of depth to basement complex is observed in profile B–B′ as illustrated in Fig. 8 hence the presence of graben structure in basement rocks enhances the contribution of faults and its associated fracture zones for connecting the Nubian aquifer to the basement rocks also the recharge of groundwater aquifer from Khour Tushka and Lake Nasser surface water as well. Fig. 9 shows the profile F–F′ was extended from southwest to northeast direction and parallel to Lake Nasser and almost perpendicular to A–A′ and B–B′ profiles. It can be notice that the depression in the ground surface which formed Khour Tushka is related to a deep structure fault that appeared in geoelectric section F–F′ and its effect occurs in the rock sedimentary cover also.

3.4. Geomagnetic measurements and results

A land geomagnetic survey was undertaken in that area to estimate the structure in the basement rock as well as the extension of these structures to the upper sedimentary covers. The

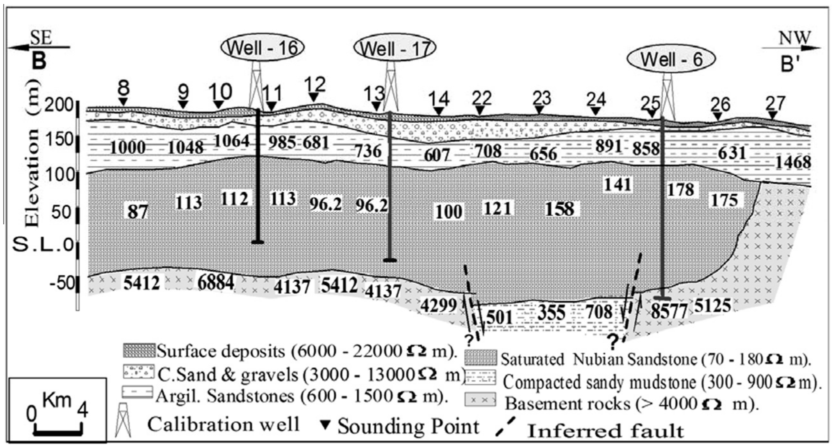

Fig. 8 Geoelectric cross section B–B′ illustrates the uplifting in basement rock due to tectonic action.

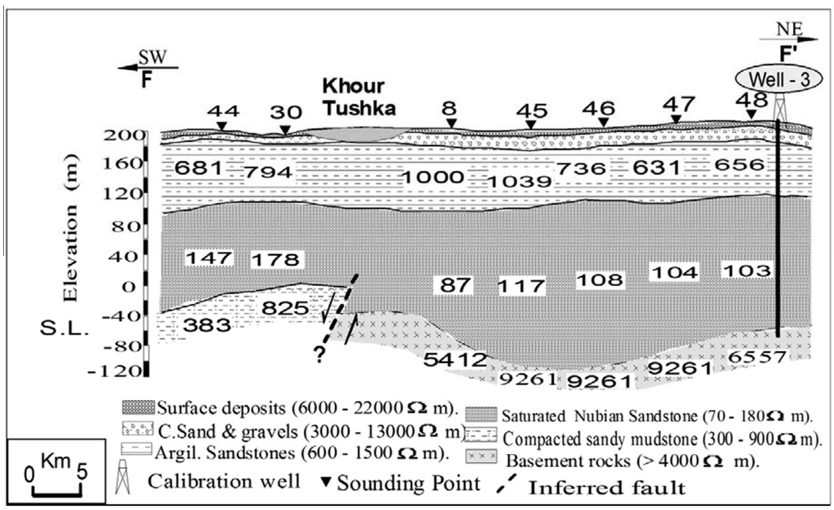

Fig. 9 Geoelectric cross section F–F′ revealing the presence of fault system extends to basement complex and connects the surface water of Nasser Lake to adjacent groundwater aquifers.

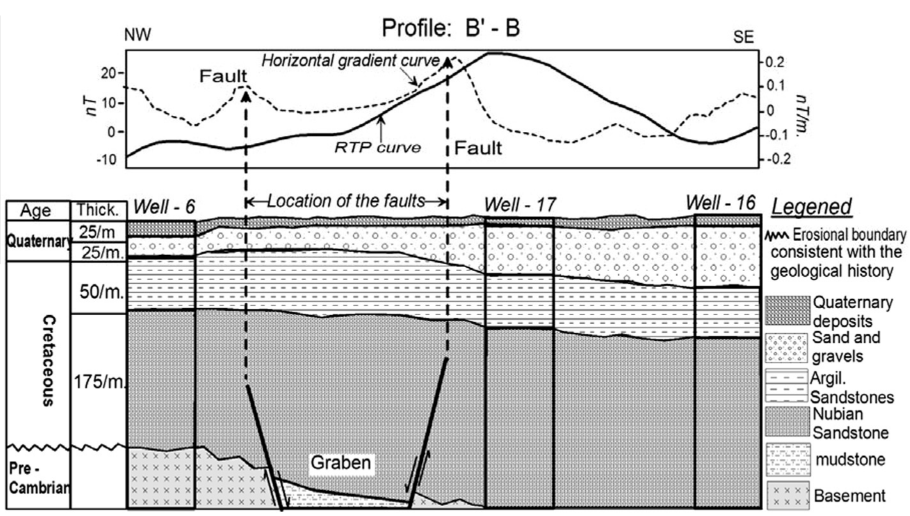

Fig. 10 Composite geologic cross section log supported by RTP magnetic profile and horizontal gradient curve along profile BB′ proposes the extension of basement structures to the upper rocks.

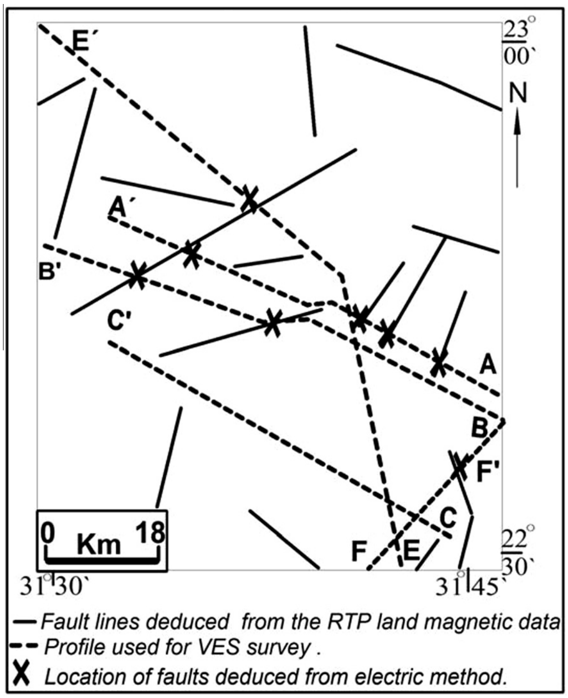

Fig. 11 Structure map deduced from the RTP land magnetic map using trend analysis shows a good correlation with the fault locations deduced from geoelectric interpretations.

geomagnetic results indicate that there is a good correlation between geologic cross sections along profile B–B′ obtained from composite well logs, RTP magnetic profiles, and horizontal gradient curves as shown in Fig. 10. This validates the trend analysis from the geoelectric interpretations, where the peaks of the horizontal gradient are correlated with the fault locations. These structure trends affect the hydraulic transmissivity of overlain groundwater aquifers and cause the later discontinuities resulting in the presence of faults and their associated fracture zones. These discontinuities control the internal recharge between aquifer bearing formations relevant to accompanied fracture zones' hydraulic transmissivity. The results of geomagnetic trend analysis also showed that the most predominant tectonic trends are N45–65E, N35–45W and NNE–SSW. The least predominant trend is the E–W tectonic trend; these may be due to local tectonic effects. From the correlation of the interpreted fault locations and water resources, it appears that the faults having a NE trend are primarily responsible for conduction and recharging of the water aquifers.

Furthermore, a correlation exists between the locations of the faults inferred along the geoelectric cross-sections and their locations from the magnetic trend analysis as shown in Fig. 11. The results indicate that these faults are caused by basement tectonics.

4. Discussion and conclusion

Subsurface fractures are not visible, thus, its characterization is a difficult task. However, the polarimetric borehole radar system is capable to maintain such an objective. In this work, we are attempting to apply the polarimetric analysis for the measured polarimetric borehole radar data, which is equivalently applied to Polarimetric Synthetic Aperture Radar (PolSAR) datasets, to determine the hydraulic characteristics of the subsurface fractures. Two different locations in USA and Egypt were selected to investigate the hydraulic transmissivity of subsurface fractures and their effect on the groundwater recharging. The first polarimetric datasets have been acquired at Mirror Lake, USA which is well known as a standard site for testing the properties of subsurface fractures. For each single polarization (e.g. VV, VH, HV, HH) entropy, anisotropy and alpha were estimated and used to characterize subsurface fractures at different frequencies (e.g. 30, 60, 80 and 100 MHz).

The results show the presence of nine fracture zones in one borehole FSE-1. We observed that high frequency components are less sensitive to evaluate the small fracture surface roughness variation; hence the depolarization effect of the electromagnetic waves gets stronger compared to that observed with low frequencies. Subsurface fractures can be differentiated into four categorized groups related to its hydraulic properties and these results showed a good consistency with the hydraulic permeability tracer test.

Similarly, the surface geophysical measurements of geoelectric and geomagnetic methods were applied to delineate the occurrences of subsurface structures around Lake Nasser. As, the hydraulic effect of fault systems and their associated fracture zones controls the water recharging from Nasser Lake to adjacent aquifers. The analysis of the surface measurements revealed that basement rocks have been affected by two predominant sets of faulting systems trending in NE and NW directions. The correlation of the locations of these faults and the water resources show that the faults having NE trend are most responsible for recharging of the groundwater aquifers and having the highest hydraulic transmissivity zones.

The polarimetric analysis based on the three eigenvector decompositions (entropy, anisotropy and alpha) for subsurface fracture characterization, figured out clear explanation of the physical properties of different subsurface fractures. The results obtained from Mirror lake site were used as key guide to evaluate hydraulic property of the subsurface structures at Lake Nasser. The results show a good correlation and a logic explanation for the prevailed subsurface structures and the recharging process at southwest Lake Nasser area.

This work is a key to help the geophysicists for further exploration of subsurface fractured aquifers and its suitability for agriculture purposes.

Acknowledgment

This work was supported by JSPS Grant-in-Aid for Scientific Research (A) 23246076.

References

Bogdanov, I.I., Mourzenko, V.V., Thovert, J.-F., Adler, P.M., 2003. Effective permeability of fractured porous media in steady state flow. Water Resour. Res. 39 (1), 1023. http://dx.doi.org/10.1029/2001WR000756.

Butzer, K.W., Hansen, C.L., 1968. Desert and River in Nubia: Geomorphology and Prehistoric Environment at Aswan Reservoir. University of Wisconsin, Madison, Wisconsin, U.S.A.

Cloude, S.R., Pottier, E., 1997. An entropy based classification scheme for land applications of polarimetric SAR. IEEE Trans. Geosci. Remote Sens. 35 (1), 68–78.

Continental Oil Company (CONOCO)., 1987. Geologic Map of Egypt (Scale 1:500,000).
Dershowitz, B., Miller, A., 1995. Dual porosity fracture flow and transport. Geophys. Res. Lett. 22, 1441–1444.
Egyptian Geological Survey and Mining Authority (EGSMA)., 1993. Geologic Map of El-Hasana Area. North Sinai, Egypt.
El Shazly, E.M., Abdel Hady, M., El Ghawaby, M., El Kassas, I.A., 1974. Geologic interpretation of ERTS-1 satellite images for west Aswan area, Egypt. In: Proceedings of the Ninth International Symposium on Remote Sensing of the Environment, 15–19 April 1974, Ann Arbor, Michigan, U.S.A, pp. 119–131.
El Shazly, E.M., Abdel Hady, M.A., El Kassas, I.A., Salman, A., El Shazly, M.M., El Amin, H., Abdel Megid, A.A., 1976. Geology of Kharga-Dakhla Oasis area, Western Desert, Egypt, from NASA land sat.1 satellite images: Remote Sensing Research Project, Acad. Sci. Res. Technol. p. 41 (Cairo, Egypt).
Ghoubashi, S., 2010. Impact of Lake Nasser on the groundwater of the Nubia sandstone aquifer system in Tushka area, South Western Desert, Egypt. J. King Saud Univ. Sci. 24, 101–109.
Hendriks, F., 1987. Die Entwicklungsgeschichte des SE-Ägyptischen Sedimentationsraumes in der Kreide und im Alttertiar: Eine Beckenstudie. Unveroff Habil.-Schrift, TU Berlin.
Issawi, B., 1968, The geology of Kurkur-Dungle area: Geol. Surv. paper No. 46, 102, Cairo, Egypt
Lane, J.W., Haeni, F.P., 1998. Use of a multi-offset borehole-radar reflection method in fractured crystalline bedrock at Mirror Lake, Grafton County, New Hampshire. In: Proc. Symp. Appl. Geophys. Eng. and Environ. Problems, pp. 359–368.
Lee, Jong.-Sen, Eric, Pottier, 2009. Polarimetric radar imaging: from basics to applications. CRC Press, Taylor and Francis.
Kazemi, H., Gilman, J.R., 1993. Multiphase flow in fractured petroleum reservoirs. In: Bear, J. et al., Flow and Contaminant Transport in Fractured Rocks, Academic, San Diego, Calif., pp. 267–323.
Khalil, M., Santos, F., Moustafa, S., Saad, U., 2009. Mapping water seepage from Lake Nasser, Egypt, using the VLF-EM method: a case study. J. Geophys. Eng. 6, 101–110.
Klitzsch, E., Wycisk, P., 1987. Geology of the sedimentary basins of Northern Sudan and bordering areas, Berliner Geowissenschaft Abhandlung (A) 75 (1), 97–136 (Berlin).
Kranz, R.L., Frankel, A.D., Engelder, T., Scholz, C.H., 1979. The permeability of whole and jointed Barre granite. Int. J. Rock Mech. Min. Sci. 16, 225–2234.
Sato, M., Takeshita, M., Miwa, T., Lane Jr., J.W., 1999. Polarimetric borehole radar measurement at the Mirror Lake test site. Proc. SPIE 3752, 104–112.
Renard, P. et al, 2001. Laboratory determination of the full permeability tensor. J. Geophys. Res. 106, 26,443–26,452.
Smith, L., Schwartz, F., 1993. Solute transport through the fracture networks. In: Bear, J. et al., Flow and Contaminant Transport in Fractured Rocks, Academic, San Diego, Calif., pp. 129–167.
Taylor, W., Pollard, D., Aydin, A., 1999. Fluid flow in discrete joint sets: field observations and numerical simulations. J. Geophys. Res. 104, 28,983–29,006.
Van Houten, F.B., Bhattacharyya, D.P., 1979. Late Cretaceous Nubia formation at Aswan south eastern desert, Egypt. Ann. Geol. Surv. Egypt 11, 408–431.
Wu, H., Pollard, D.D., 1995. An experimental study of the relationship between joint spacing and layer thickness. J. Struct. 17 (887–17), 905.
Wu, H., Pollard, D.D., 2003. Imaging 3D fracture networks around boreholes. AAPG Bull. 86, 593–604.